ISTITUTO NAZIONALE DI FISICA NUCLEARE

Sezione di Genova

INFN/FM-90/4
26 Novembre 1990

F. Parodi, R. Vaccarone:

THE CRITICAL STATE AND THE FLUX DYNAMICS IN SQUID ARRAYS

Servizio Documentazione
dei Laboratori Nazionali di Frascati

INFN - Istituto Nazionale di Fisica Nucleare
Sezione di Genova

INFN/FM-90/4
26 Novembre 1990

THE CRITICAL STATE AND THE FLUX DYNAMICS IN SQUID ARRAYS

F. Parodi and R. Vaccarone
I.N.F.N., Sezione di Genova
Via Dodecaneso 33, 16146 GENOA, ITALY

ABSTRACT

The low transport current in granular High T_c superconductors is undoubtely attributed to the presence of weak links between grains. Magnetization and critical current measurements at very low field indicates that this low transport current behaves as expected from a critical state model.
In this paper we show that a simple linear model of the granular system, based on an array of Josephson Junctions and holes, can explain the existence of the critical state regime and shows dynamical effects, which have consequences even at low frequency, allowing for instance to explain the flux flow resistance of these materials.

1. Introduction.

Most of the High T_c superconductors are easily prepared in the form of granular aggregates by a sintering process. In such systems the grains have good superconducting properties and below some low critical field H_{c1} present a complete Meissner effect. The surface of separation between the grains is the weak point for the transport current, showing a critical current orders of magnitude lower than the grains. Anyway the material as a whole still shows superconducting properties. The junctions between the grains are superconducting weak links and show Josephson character, as nicely demonstrated in [1]. Even in the mate-

rials with high density a number of voids is left between the grains and we must consider these holes as an important part in studiing the low field behaviour of these materials. To enphasize this aspect we prefer to model the system as an array of SQUIDs, rather than a network of junctions [2].

The system is truly tridimensional and with a very high disorder. We expect that in such a complex network nor the current can follow a regular straight path nor the field can be described by a twodimensional map.

However in this paper we use a simple, onedimensional and regular model to show the possibility to describe such a system by a macroscopic critical state model, and to analize also the dynamic of the flux inside the material.

A further simplification is also introduced, by treating the junctions as point-like, and so we can only obtain a macroscopic behaviour equivalent to the Bean model [3]. The effect of finite junction length in the same system has been treated in [4].

A linear array of Josephson junctions has been studied by Yamashita et al. [5] by means of a mechanical analog. Pinning has been detected but the critical state has not been searched. Networks of junctions in two dimensions have been studied by many authors [6,7], but all of them have neglected the effect of the self field and by this choice they where not able to obtain information about the existence of a critical state in the system.

Our linear model describes a real system called quantum flux shuttle which has been studied to develop shift registers in Josephson computers [8]. For these devices it is necessary to work with well separated non interacting fluxons and a piling up of fluxons as in a critical state regime must be avoided.

2. The one dimensional SQUID array.

A linear array of SQUIDs will describe two ideal superconducting electrodes connected at discrete points by Josephson Junctions, which we consider in the following pointlike. A finite area remains in between two adjacent junctions and the two electrodes and the whole system can be seen as a multihole SQUID.

This linear array of josephson junctions separated by voids is described by the discrete sine-Gordon equation, to which we must add a dissipative term:

$$\varphi_{n+1} - 2 \cdot \varphi_n + \varphi_{n-1} = \gamma \frac{\partial^2 \varphi_n}{\partial t^2} + \beta \cdot sin(\varphi_n) + \eta \frac{\partial \varphi_n}{\partial t} \qquad (1)$$

The phase φ_n is the phase difference between the two superconducting electrodes at the junction n and its increment between adjacent junctions is proportional to the magnetic flux in the hole. The coefficients γ , β and η are given by:

$$\gamma = \mu_0 C S_{hole} \qquad (2a)$$

$$\beta = \frac{2\pi \mu_0 S_{hole} I_m}{\Phi_0} \qquad (2b)$$

$$\eta = \frac{\mu_0 S_{hole}}{R} \qquad (2c)$$

where C and R are the junction capacitance and shunt resistance and I_m is the maximum Josephson current; S_{hole} is the hole area and $\mu_0 S_{hole}$ is equivalent to the self inductance of the loop encircling the hole. Both I_m, C, R and L are calculated per unit length along the field direction.

Considering granular YBCO we can assume a grain size of 10 μm, hole areas ranging from $S_{hole} = 3 \times 3\mu m^2$ to $1 \times 1\mu m^2$, and $J_c = 200A/cm^2$ at 77 K to $15KA/cm^2$ at 4.2 K giving $I_m = 20 \div 1500A/m$. We obtain a resistance $R = 10^{-5}\Omega/m$, starting from a typical resistivity of $1\, m\Omega\, cm$. The capacitance C is about 1. 10^{-8} F for an oxide barrier 50 $\mathring{A}$ thick, but can be orders of magnitude lower for S-N-S junctions.

In the static case the equation reduces to:

$$\varphi_{n+1} - 2 \cdot \varphi_n + \varphi_{n-1} = \beta \cdot sin(\varphi_n) \tag{3}$$

The solution of this equation resemble closely the analogous case of an uniform junction, but the discretness in space is the cause of pinning and will allow the system to stay in a critical state.

As in the continuous case (see Owens and Scalapino [9]) we can find a group of solutions with zero internal field. These consists of a regular array of fluxon - antifluxon pairs. We can label these solution by their period N and by the number M of $\Phi - \bar{\Phi}$ pairs contained in this period. Of course the period cannot be smaller than $N = 2$ with $M = 1$.

The solutions with nonzero (positive) internal field are given by a regular array of fluxons.

In this case the average internal field is given by $f = M/N$ where N is the period of the solution and M the number of fluxons in this period.

These two classes of solutions resemble closely the field profiles found in the case of a continuous junction if the field is low ($f \ll \frac{1}{2}$) and $\beta \ll 2\pi$. The half width of a fluxon is given by $\lambda_{array} = \beta^{-\frac{1}{2}}$ at low βs but it should tend asymptotically toward $\sim .25$ even for $\beta \to \infty$ because at high βs a flux quantum will be contained in a single hole (for fluxons centered on the hole itself). If the fluxon is centered on a junction it will be shared between two holes and its half width will tend to .5 . This dependence of λ_{array} on β is shown in figure 1.

Moreover, the solution with $f \neq 0$ will degenerate at $f = \frac{1}{2}$ in a constant field profile ($h_n = \frac{1}{2}$). For $-\frac{1}{2} < f < 0$ the field is given by the negative of the previously found solution. The field profiles at any f can be obtained from those at $-\frac{1}{2} < f < \frac{1}{2}$ by summing an integer K to the solutions previously found .

$$h_n^f = h_n^{f-K} + K \tag{4}$$

The phase can be obtained by adding a linear term $K \cdot n$ to the restricted zone solution while the current is periodic in field ($I_n^f = I_n^{f-K}$). Even the zero field solution can be extended including solutions with K fluxons per hole plus an array of fluxon - antifluxon pairs.

3. Flux pinning.

While in an homogeneous infinite junction a static fluxon can stay in equilibrium at every x, the discrete array has preferred sites (the holes) in which the fluxon will be in stable equilibrium.

The energy density of an array of junctions and holes consists of two terms: a magnetic one e_m due to the magnetic field in the hole and e_J coming from the current flowing in the junction. The total energy density (in reduced units) is given by:

$$e = e_m + e_J = \frac{(\varphi_n - \varphi_{n-1})^2}{2} + \beta \cdot (1 - cos(\varphi_n)) \tag{5}$$

The reduced energy of an insulated fluxon is obtained by integrating in space this energy density.

The fluxon energy has a minimum when the fluxon is centered in an hole and a maximum when it is centered on a junction. The energy difference between these two cases is the energy barrier the fluxon has to overcame to jump from one hole to the next one.

The value of this barrier energy has been calculated as a function of β and its behaviour is shown in Fig. 2.

The barrier energy decreases steeply when β decreases below $\sim 2..$ We will see later thath also the critical current decreases strongly at about the same value.

The β values for granular YBCO with the standard parameters given before, ranges from $\beta_{min} \sim .08$ to $\beta_{Max} \sim 50$.

The pinning energy can be obtained from the reduced energy equation 5 by:

$$\Delta E = \frac{L_{grain}}{\mu_0 \cdot S_{hole}} \cdot \left(\frac{\Phi_o}{2\mu_0}\right)^2 \cdot \Delta e = \alpha \cdot \Delta e \tag{6}$$

In a typical granular sample with holes of area $4.10^{-12} m^2$ and a grain size of $10.\mu m$ the costant α is 2.10^{-19} joules.

Comparing the barrier energy with the termal energy KT we can see that at 77. K the termal energy overcomes the pinning energy at $\beta \sim 1.$ while at 4.2 K the same crossing happens at $\beta \sim .5$.

The energy barrier has been calculated for an insulated fluxon at zero internal field and zero field gradient. This energy is $U_0(0)$, the pinning energy at zero field.

Unfortunaly we cannot calculate exactly this same energy if $f \neq 0$ and/or a field gradient exists.

When an internal field and a field gradient exist, it is quite difficult to associate an energy barrier to the movement of a single fluxon, or to find the pinning force acting on it. In fact the whole flux distribution is correlated and many different flux distributions can share almost equal local field and field gradient but have different stability with respect to a fluxon displacement.

4. Critical state.

The search for a critical state regime consists in finding the solutions of our equation with the maximum magnetic field gradient. The solution cannot be obtained by treating a single fluxon, because the pinning strenght depends on field in a periodic way and we must calculate the field gradient over one field period. The same conditions are reproduced every time one more fluxon is present in every cell of the array.

To simplifie the writing we express from now on β and φ in units of 2π :

$$\bar{\beta} = \frac{\beta}{2\pi} \qquad \bar{\varphi} = \frac{\varphi}{2\pi} \tag{7}$$

It is very simple to find a critical state profile when $\bar{\beta}$ has an integer value.

If $\bar{\beta} = K$ the phase $\bar{\varphi}_n$ of the junction will be given by

$$\bar{\varphi}_n = K \cdot \frac{n(n+1)}{2} + \frac{1}{4} \tag{8}$$

which gives an uniform critical current $I_{cn} = K$.

If $\bar{\beta} > 1$ we can find solutions with a critical current $I_{cn} = Int(\bar{\beta})$ and a phase given by

$$\bar{\varphi}_n = K \cdot \frac{n(n+1)}{2} + \frac{asin(\frac{Int(\bar{\beta})}{\bar{\beta}})}{2\pi} \tag{9}$$

but we must verifie if this critical current is the maximum one. Indeed in this case any junction will carry an uniform current lower than its maximum.

When we have $\bar{\beta} < 1$ it is not possible to have an homogeneous current in the array. However we want to show that a critical state regime still exists.

We must first of all define the critical current itself by deciding over which length we must average the local current and the choice can be that to consider a field period. Indeed we can find a state with a field gradient in the array with the following characteristics:

1) The current in the junctions is periodic in space with a period T_N and with as an average value given by a rational number $\langle I \rangle = M/N$.
2) The field has a linear gradient plus a periodic correction with the same period.
3) The phase is quadratic in space plus a periodic correction.

To obtain these solutions we can split the reduced phase in a quadratic term φ_n^* and a periodic one $\delta\varphi_n$.

The quadratic term can be written as:

$$\varphi_n^* = \frac{n \cdot (M \cdot n + M \cdot N + 2 \cdot L)}{2 \cdot N} \tag{10}$$

The phase correction $\delta\varphi_n$ can be obtained from the Sine Gordon equation with periodic boundary conditions. The period T_N is equal to N. We obtain the following equation where the coefficient a_n and b_n are both periodic.

$$\delta\varphi_{n+1} - 2\delta\varphi_n + \delta\varphi_{n-1} = \bar{\beta} \cdot (a_n \cdot cos(2\,\pi\delta\varphi_n) + b_n \cdot sin(2\,\pi\delta\varphi_n)) - M/N \quad (11)$$

with

$$a_n = sin(2\,\pi\varphi_n^*) \qquad \text{and} \qquad b_n = cos(2\,\pi\varphi_n^*) \quad (12)$$

$\delta\varphi_n$ being periodic, the average over one period of the current in the array does not depend on the solution found and can be obtained simply from the quadratic term φ_n.

By changing the parameter L in the sequence φ_n we can shift the field profile in space. The profile will shift of one complete cell if L changes by M. By a proper choice of L we can find sequences af a_n and b_n which are both periodic and symmetrical. If the solution of equation 11 is symmetrical too we get a symmetrical current distribution and an antisymmetrical field profile.

Depending on N and M the symmetry point can be an hole or a junction. In the former case the field at this hole will be a multiple of M while in the latter the holes adjacent to the central junction will have fields above and below M by an equal amount. A second simmetry point is found at the center of the sequence (again on a junction or on an hole).

The search for the critical state solution requires to find the maximum average current in the array as a function of β. The same result can be obtained by looking for the minimum $\bar{\beta}$ value which allows solutions of equation 11 at any rational value of J_c ($= \langle I \rangle_c$).

The numerical procedure consists in solving the system of trascendal equations given by equation 11 for $n = 0 \div N - 1$ with the constraints

$$\delta\varphi_{-1} = \delta\varphi_{N-1} \qquad \text{and} \qquad \delta\varphi_N = \delta\varphi_0 \quad (13)$$

For any J_c and any $\bar{\beta}$ we can find more than one solution of the system of equations. Starting from high $\bar{\beta}$ values we can find numerically some of this solutions and then we reduce gradually the $\bar{\beta}$ using the previously found solutions as a starting point for the new case to help convergence. At some intermediate points more and more solutions does not converge anymore and we are left with two solutions wich at $\bar{\beta}_{min}$ coincide. Moreover we note that at $\bar{\beta}_{min}$ the solutions are symmetrical.

This solutions has been found for a number of J_c ranging from 1/36 to 8/9 and J_c vs $\bar{\beta}$ is shown in fig. 3.

Even a few solutions with $J_c > 1$ and $\bar{\beta} > 1$ are shown in the same figure.

The main result of such a calculation is that we could not find a regular curve to describe the critical current versus $\bar{\beta}$ behaviour. This is due to the difficulty to accomodate an integer number of fluxon in a finite number of holes. However we can show that the current density is almost everywhere lower than $\bar{\beta}^2$ save at $\bar{\beta} = M$ and at some special points (i.e. $J_c = 1/2, 1/3, 2/3$).

The morfology of the field profile is complex and we can find a regular trend only in same regions. In figure 4 and 5 we show the field profiles at $\bar{\beta}_{min}$ and $J_c = 1/N$. In figure 4 a and 4 b we observe that the field gradient has a minimum near to the symmetry point where the flux is an integer multiple of Φ_0 and in particular at low J_cs we see individual fluxons gathered around $\Phi_0/2$. In figure 5 we show the field profiles with J_c near 1. We can observe in the curves having higher J_c that the current is near its maximum in almost all the junctions.

5. The build-up and the evolution of the critical state

The previous solutions will not solve the real problem of a finite sample with arbitrary boundary conditions. The periodic solutions can assume only a finite number of values at the sample ends. Moreover in a sample with externally applied field we expect a reversal of the current in the sample center and even in a sample with transport current alone we must find solutions with $J = J_c$ and $J = 0.$ in different places.

We want to show that the critical state is attained for any cycle of field and current, that regions with no current and with positive and negative current density can coexist and that the critical current density will assume the maximum value which has been previously calculated.

To get this result we must solve the system of time dependent equations given in formula 1 with boundary conditions for the external field at the sample sides ($B_0 = B_N = B_{ext}$ for magnetization or $B_0 = -B_N = I/N$ for simulation of transport current).

B_{ext} or I will depend on time and the evolution of the field profile can be obtained, together with the total internal field (magnetization case) or the voltage on the sample (transport current case).

We rewrite here the system of equation 1 with the phase normalized to 2π, $\bar{\beta} = \beta/(2\pi)$ and the time normalized to a characteristic time given by

$$\tau_0 = \sqrt{\gamma} \tag{14a}$$

The coefficient of the dissipative term becomes

$$\bar{\eta} = \eta/\sqrt{\gamma} \tag{14b}$$

The resulting equation is:

$$\bar{\varphi}_{n+1} - 2 \cdot \bar{\varphi}_n + \bar{\varphi}_{n-1} = \frac{\partial^2 \bar{\varphi}_n}{\partial \tau^2} + \bar{\beta} \cdot sin(2\pi\bar{\varphi}_n) + \bar{\eta}\frac{\partial \bar{\varphi}_n}{\partial \tau} \tag{15}$$

The time evolution of the internal field has a time scale which is given by τ_0 and the parameters governing this evolution are the hysteresis parameter $\bar{\beta}$ and the damping constant $\bar{\eta}$.

In a HTSC material with standard grain size, density and junctions properties we can assume a $\gamma = 10^{-26} \div 2 \cdot 10^{-25}$ and a damping parameter $\eta = 10^{-13} \div 10^{-12}$. So the time scale is $\tau_0 = 10^{-13} \div 4 \cdot 10^{-13}$ and the reduced damping factor $\bar{\eta}$ ranges from 10. to 30.

If the external field (or current) variation is very slow compared with τ_0 we get a quasi static solution which will consist of a sequence of stable field profiles and sudden transitions in between. This behaviour is obtained only in the case of damping factor $\bar{\eta} \geq \pi$.

We solved equation 15 for a number of $\bar{\beta}$ values ranging from .35 to 2. with the boundary conditions describing a transport current. The results correspond exactly to a critical state solution and we can get the critical current density in the sample. These data are shown in figure 6.

The J_c vs $\bar{\beta}$ curve is almost identical to that presented in figure 3 and obtained from periodic solutions in an infinite sample.

In figure 7 we show a number of field profiles for different $\bar{\beta}$ and in figure 8 some profiles at different times during a magnetization cycle obtained by the numerical simulation. It is clear that the field profiles are almost identical to the corresponding ones of the periodic case, even if in the present case the field gradient is coexisting with zones at zero field or with an opposite gradient. So the Bean model of the critical state is followed very well by our system.

In the case of system simulating a sample with transport current we can obtain the electric field along the sample (or the electric potential) by:

$$v = \frac{\partial \bar{\varphi}_0}{\partial \tau} \tag{16}$$

This potential shows a sequence of spikes in correspondence with the entrance of a new flux quantum in the sample. The time width of such spikes is of the order of γ.

When simulating magnetization a similar phenomenon is observed. The internal flux, which is obtained from:

$$\frac{\Phi_{int}}{\Phi_0} = \bar{\varphi}_N - \bar{\varphi}_0 \tag{17}$$

follows the standard curve expected from the Bean model, but the separated entrance of any fluxon is seen as steps of one flux quantum.

The damping parameter causes even larger effects on the overall behaviour at larger times. We can observe that equation 15 is a nonlinear discrete wave equation with a damping term. When $\bar{\eta}$ is large and the time variation is slow we can neglect the $\varphi_{\tau\tau}$ term such that the remaining equation acquires the form of a diffusion equation. On the contrary for low $\bar{\eta}$ values the wave character of the equation predominates. This last situation is unlikely in real samples with the physical parameters given before.

In the case of high damping the flux enters or escape from the sample with some delay and the profile reachs only asimptotically the linear profile of the static solution. From our numerical simulation we obtain that only if the field applied to the sample changes with a rate lower than

$$\frac{\partial B_{ext}}{\partial t} = S_{hole}\, \Phi_0\, \frac{\eta}{\gamma} {N_p}^2 \tag{18}$$

the field evolution is quasi-static. Significant transient effects can be seen only at microwave frequencies.

This empirical formula can be explained by the fact that a fluxon will move in the array traveling a cell length in a time η and the increase of the flux on the side of the sample by a flux quantum corresponds to the entrance of N_p fluxons

which must travel $N_p/2$ cells to reach an equilibrium point. N_p is the number of cells which are reached by the magnetic field (penetration depth).

The change of the hysteresis cycle due to different damping factors at very high frequency is shown in figure 9.

7. Flux flow

When a superconducting sample with a finite critical current density and which follows the critical state model is completely penetrated by the transport current it will develop a finite voltage even in steady state conditions because of the flux flow phenomenon.

Indeed the current density in the sample will be anywhere equal to the critical current density and no static solution can be found for a total current greater than $I_c = J_c \cdot w$ where w is the sample width.

In our model of a linear SQUID array we must observe that the current density in the array is equal to the critical one obtained by equation 11 even if current has not fully penetrated the sample. When the critical current is reached the periodic solutions we have found will extend over the whole array. To look for a current higher than the critical means to search at a fixed β a solution with J_c higher than that shown in figure 3, which is of course impossible. But time dependent solutions of equation 1 are possible even for $J > J_c$.

These solutions are composed by a phase component increasing linearly in time, which will be seen as a finite voltage over the sample and in a movement of fluxons traveling from one to the other side of the sample itself.

The sample potential increases linearly for $I > I_c$ with a dynamic flux flow resistance equal to R. At the same time the flow velocity of the fluxons increases. This nonlinear resistive curve is shown in figure 10. The noise in the curves is due to a non complete filtering of the spikes due to the fluxon entrance.

6. Conclusions

In this paper we have shown that the transport current and the magnetic field behaviour of a granular superconducting system can be described by a critical state model and that this model will derive directly from an elementary description of the system as an array of Josephson Junctions separated by holes. To obtain such a result we had not to include any distribution of the junctions or holes properties.

The overall critical current density depends on the critical current current of the Josephson Junctions forming the array, but is lower than it, save at some special points, and show a complex behaviour which has been related to a coherent pinning of the fluxons. Such a structure can be easily averaged by a statistical distribution of the cell parameters.

We considered not only static effects, but even the dynamic behaviour of the system. A damping coefficient has been introduced, which at high frequencies can give additional losses beyond the hysteretic ones. A critical rate of field change for quasi-static behaviour has been also suggested.

The simulation of a sample carrying a transport current brings to the development of a flux flow resistance at currents higher than the critical one.

References

1. P. Chaudhari, J. Mannhart, D. Dimos, C. C. Tsuei, J. Chi, M. M. Oprysko and M. Scheurmann, *Phys. Rev. Lett.* **60** (1988) 1653
2. V. Calzona, M.R. Cimberle, C. Ferdeghini, F. Pupella, M. Putti, C. Rizzuto, A. Siri and R. Vaccarone, *Cryogenics* **30** (1990) 569
3. C. P. Bean, *Rev. Mod. Phys.* **36** (1964) 31
4. R. Vaccarone, *Proc. 3rd National Meeting on High Temperature Superconductivity*, Feb. 12-14, 1990, Genoa, Italy, p. 346
5. T. Yamashita and L. Rinderer, *J. Low Temp. Phys.* **21** (1975) 153
6. A. Giannelli and C. Giovannella, *Proc. 3rd National Meeting on High Temperature Superconductivity*, Feb. 12-14, 1990, Genoa, Italy, p. 358
7. C. J. Lobb, D. W. Abraham and M. Tinkham, *Phys. Rev. B* **27** (1983) 150
8. T. A. Fulton,R. C. Dynes and P. W. Anderson, *Proc. IEEE* **61**, (1973),28
9. C. S. Owen and D. J. Scalapino, *Phys. Rev.* **164** (1967) 538

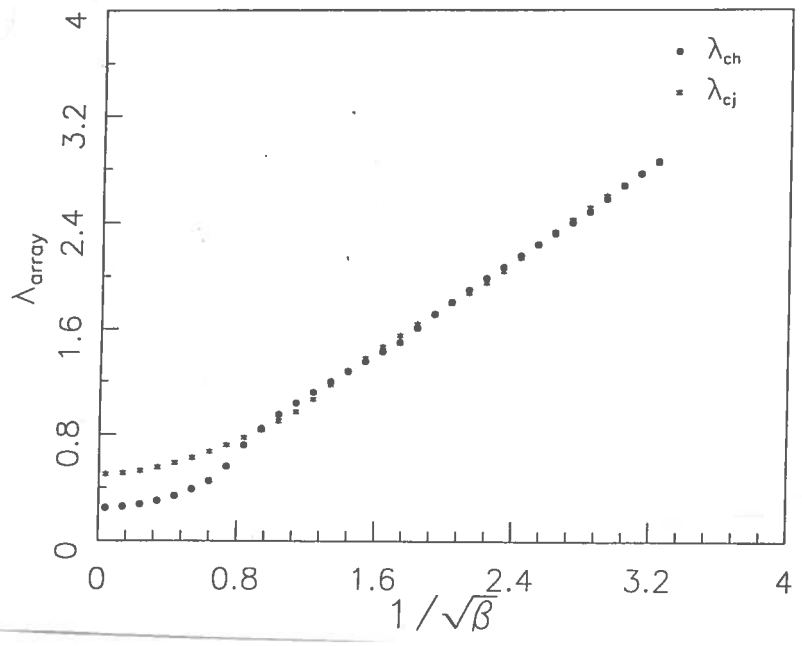

FIGURE 1.

The dependence of the penetration depth in an array of SQUIDs λ_{array} on the parameter β. The values for a fluxon centered on an hole (λ_{ch}) or on a junction (λ_{cj}) are given.

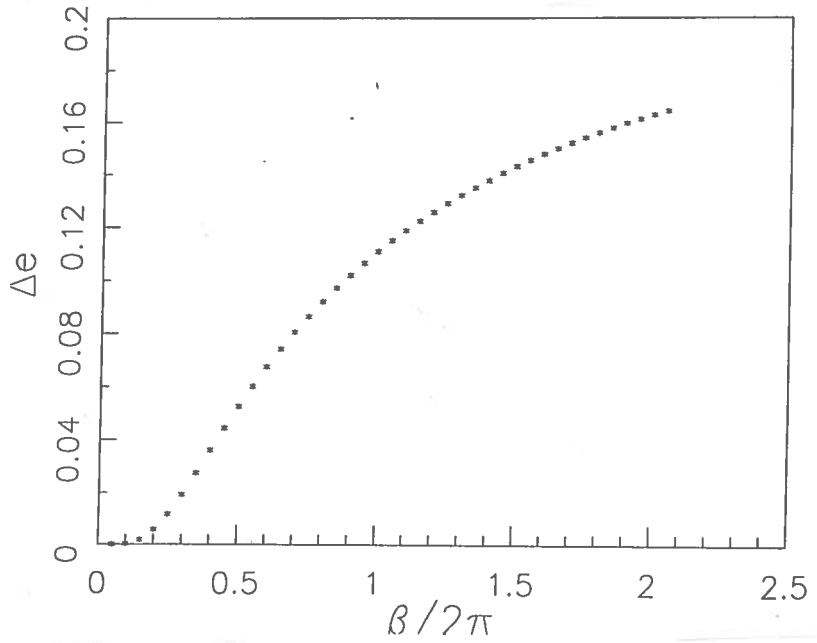

FIGURE 2.

The reduced barrier energy of an insulated fluxon Δe versus $\beta / 2\pi$.

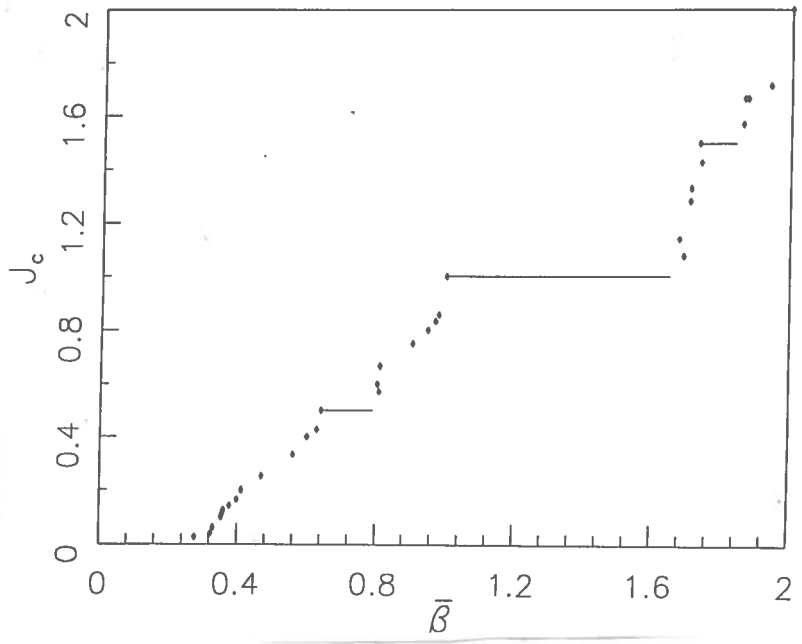

FIGURE 3.

The critical current of an array of SQUIDs as a function of $\bar{\beta}$. The line segments in the graph represent a range of $\bar{\beta}$ having the same J_c.

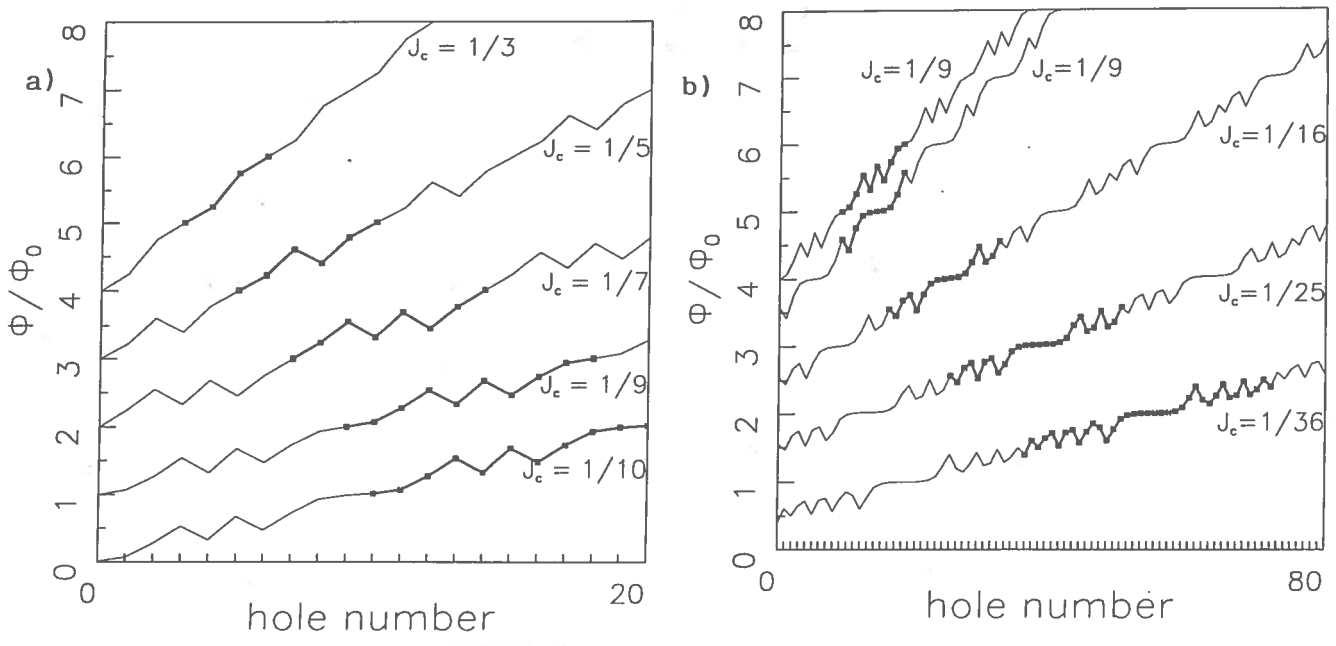

FIGURE 4.

The field profiles in the array at rational values of the critical current density: a) critical current between 1 / 3 and 1 / 10; b) critical currents between 1 /9 and 1 / 36.

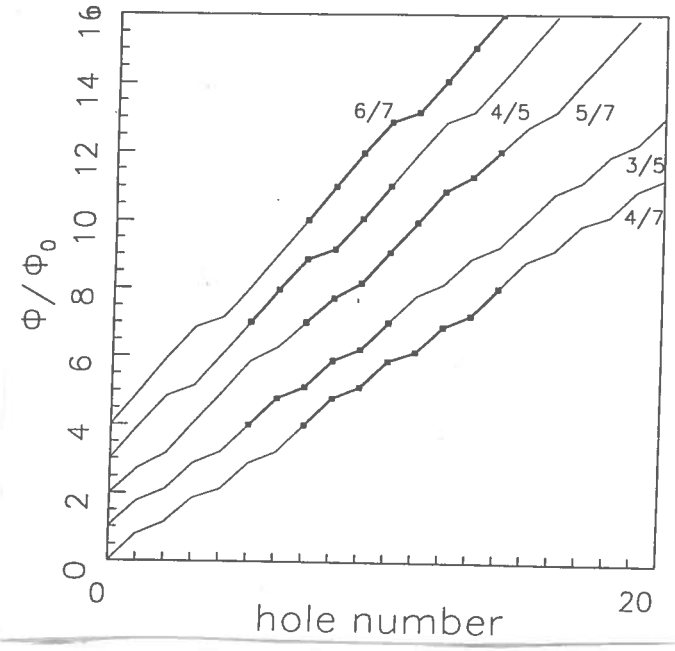

FIGURE 5.
The field profiles in the SQUID array for J_c going from 4 / 7 to 6 / 7.

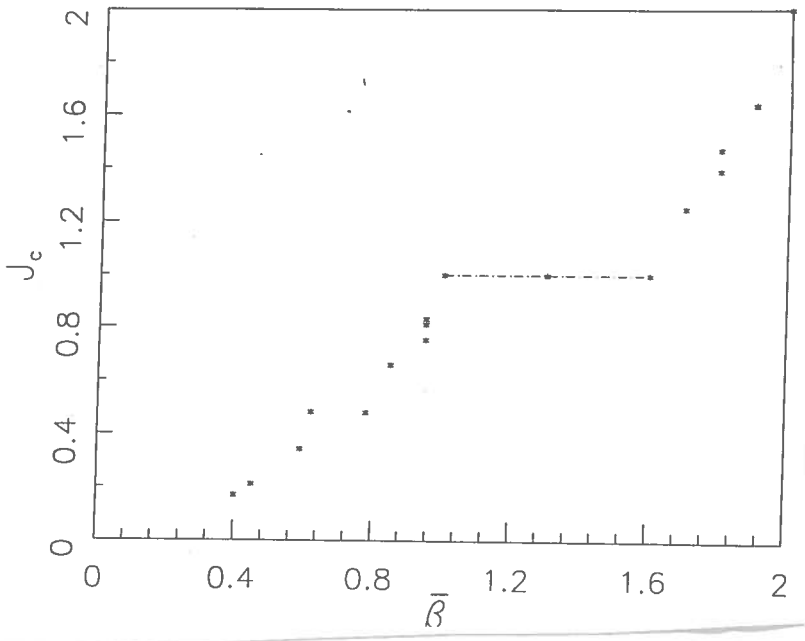

FIGURE 6.
The critical current density J_c vs $\bar{\beta}$ obtained by solving the time dependent differential equation.

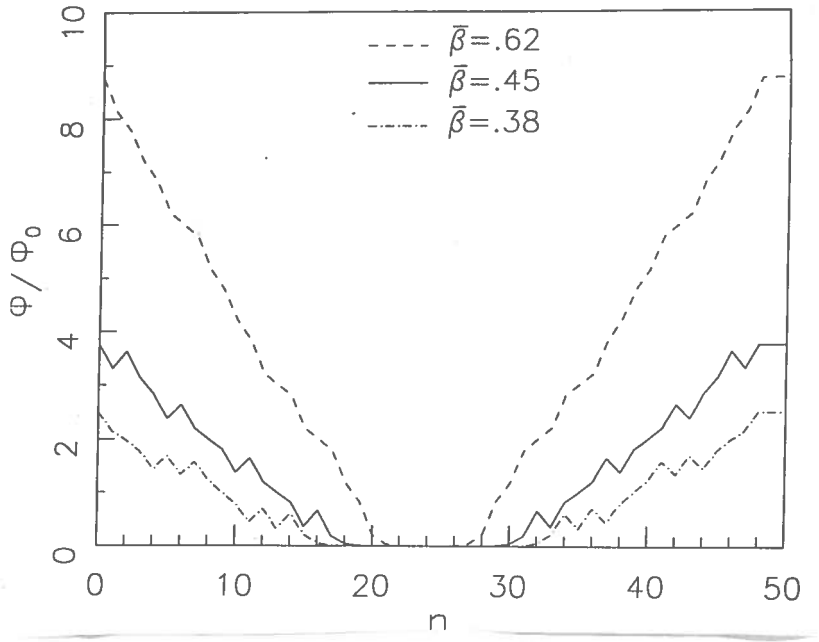

FIGURE 7.
Field profiles at different $\bar{\beta}$s.

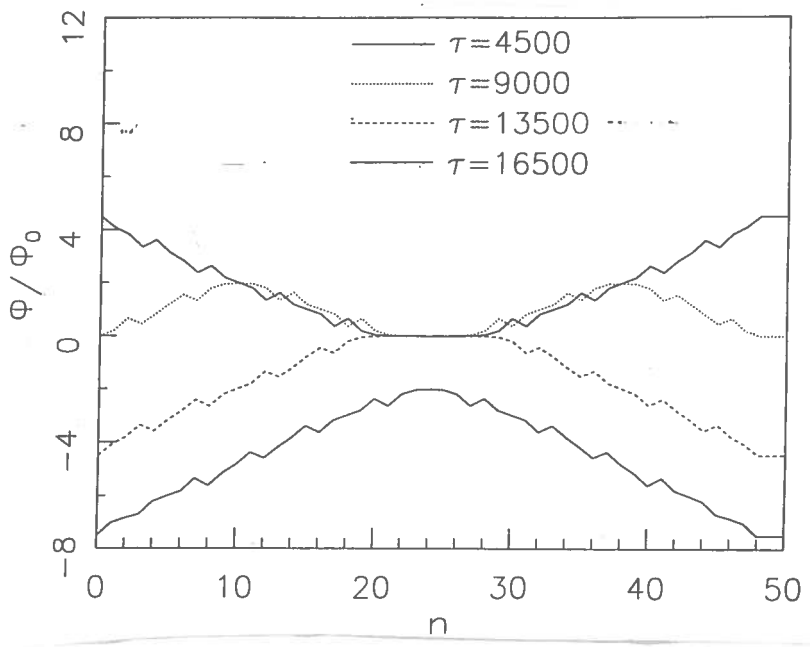

FIGURE 8.
Field profiles at different external fields during a magnetization cycle.

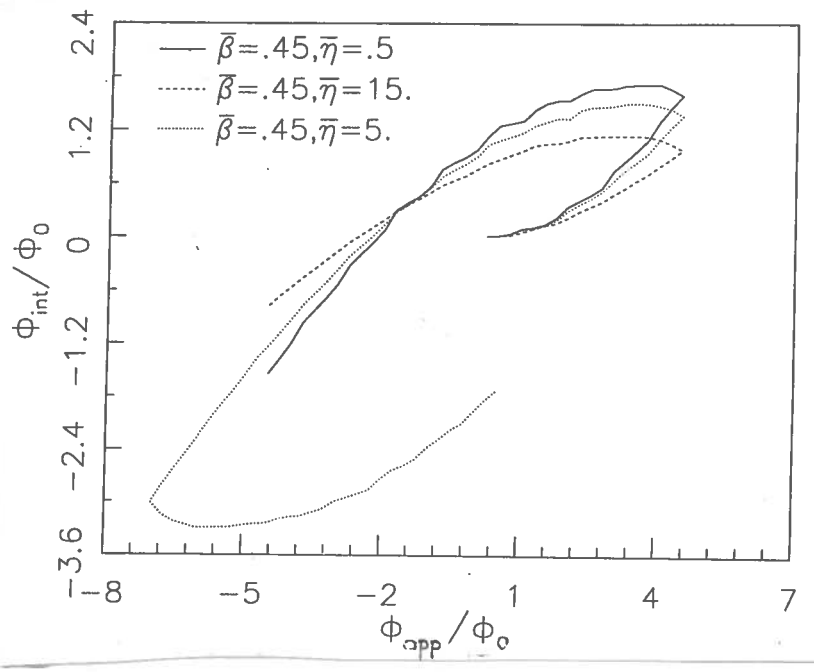

FIGURE 9.

Part of an hysteresis cycle at high frequency. The field increases and decreases linearly in time. The field increases at first from zero and the ramp is reversed before reaching the penetration field.

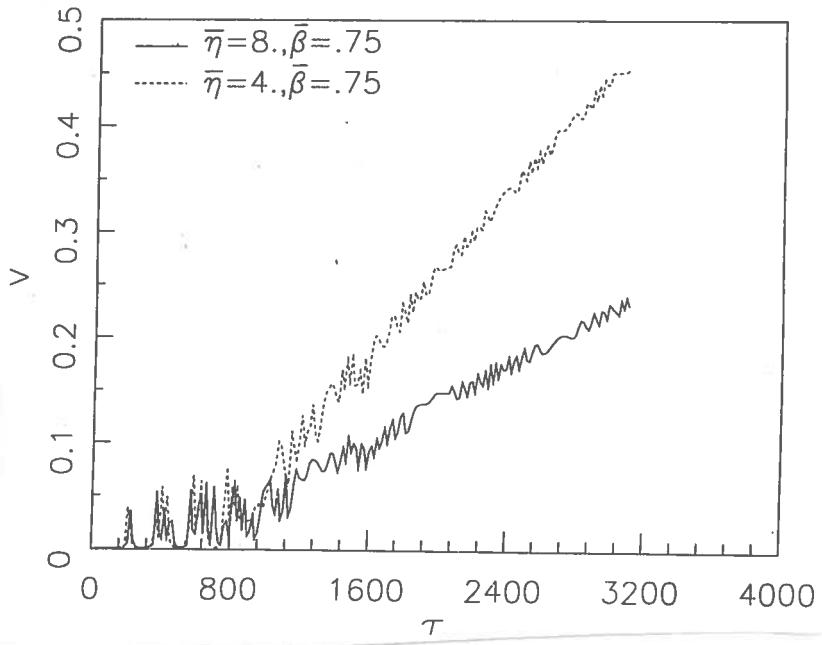

FIGURE 10.

Two examples of flux flow resistance at different $\bar{\eta}$.